Cell Reports
Report

IRF8 Is a Critical Transcription Factor for Transforming Microglia into a Reactive Phenotype

Takahiro Masuda,[1,4] Makoto Tsuda,[1,4,*] Ryohei Yoshinaga,[1] Hidetoshi Tozaki-Saitoh,[1] Keiko Ozato,[2] Tomohiko Tamura,[3] and Kazuhide Inoue[1,*]
[1]Department of Molecular and System Pharmacology, Graduate School of Pharmaceutical Sciences, Kyushu University, 3-1-1 Maidashi, Higashi-ku, Fukuoka, Fukuoka 812-8582, Japan
[2]Program in Genomics of Differentiation, National Institute of Child Health and Human Development, National Institutes of Health, Bethesda, MD 20892, USA
[3]Department of Immunology, Graduate School of Medicine, Yokohama City University, Yokohama 236-0004, Japan
[4]These authors contributed equally to this work
*Correspondence: tsuda@phar.kyushu-u.ac.jp (M.T.), inoue@phar.kyushu-u.ac.jp (K.I.)
DOI 10.1016/j.celrep.2012.02.014

SUMMARY

Microglia become activated by multiple types of damage in the nervous system and play essential roles in neuronal pathologies. However, how microglia transform into reactive phenotypes is poorly understood. Here, we identify the transcription factor interferon regulatory factor 8 (IRF8) as a critical regulator of reactive microglia. Within the spinal cord, IRF8 expression was normally low; however, the expression was markedly upregulated in microglia, but not in neurons or astrocytes, after peripheral nerve injury (PNI). IRF8 overexpression in cultured microglia promoted the transcription of genes associated with reactive states; conversely, IRF8 deficiency prevented these gene expressions in the spinal cord following PNI. Furthermore, IRF8-deficient mice were resistant to neuropathic pain, a common sequela of PNI, and transferring IRF8-overexpressing microglia spinally to normal mice produced pain. Therefore, IRF8 may activate a program of gene expression that transforms microglia into a reactive phenotype. Our findings provide a newly observed mechanism for microglial activation.

INTRODUCTION

Microglial cells are the resident immune-related glial cells of the central nervous system (CNS) that are crucial for maintaining homeostasis and sensing pathological alterations in the nervous system, such as following infection and injury (Glass et al., 2010; Hanisch and Kettenmann, 2007; Perry et al., 2010; Ransohoff and Cardona, 2010). Under normal conditions, microglia survey the surrounding local environment by actively moving their branched processes. As a consequence of multiple types of damage in the nervous system, microglia transform to reactive states through a progressive series of cellular and molecular changes, including morphological hypertrophy, proliferation and expression of various genes. In particular, expression of cell-surface receptors (e.g., toll-like receptors [TLRs] and nucleotide receptors [P2X and P2Y receptors]) and proinflammatory cytokines (e.g., interleukin [IL]-1β) is a critical process for inducing reactive phenotypes of microglia linked to the pathogenesis of various CNS diseases such as multiple sclerosis, Alzheimer's disease, and neuropathic pain (Glass et al., 2010; Inoue and Tsuda, 2009; McMahon and Malcangio, 2009; Perry et al., 2010). However, the molecular mechanisms by which microglia switch to reactive phenotypes are poorly understood.

RESULTS AND DISCUSSION

As microglia can transform into reactive phenotypes through the activation of gene transcription, we considered that reactive states of microglia may be controlled by transcription factors. To investigate this possibility, we performed a genome-wide screen of mRNAs from the spinal cord of mice with or without peripheral nerve injury (PNI), a model of CNS pathology in which remote injury of a peripheral nerve (fourth lumbar [L4] spinal nerve) results in activation of microglia in the spinal dorsal horn where the injured nerve projects. In three independent DNA microarray analyses, we identified interferon regulatory factor 8 (IRF8) as a transcription factor whose expression was significantly upregulated in the spinal cord after PNI ($p = 0.015$, Figure S1A). IRF8 is a member of the IRF family (IRF1-9), and is expressed in immune cells such as lymphocytes and dendritic cells. In the periphery, IRF8 plays pivotal roles in the immune system (Honda and Taniguchi, 2006; Tamura et al., 2000, 2008), but its role in the CNS is entirely unknown. Thus, we determined the type of cells expressing IRF8 in the spinal cord after PNI using an immunofluorescence approach. Three days after PNI, on sections from the L4 spinal dorsal horn, we observed strong immunofluorescence of IRF8 protein dotted on the ipsilateral side (Figure 1A). In contrast, on the contralateral side where intact nerves project, IRF8 immunofluorescence was weak. The observed staining was not a nonspecific signal because no IRF8 immunofluorescence was detected in mice lacking IRF8 (*Irf8*$^{-/-}$)

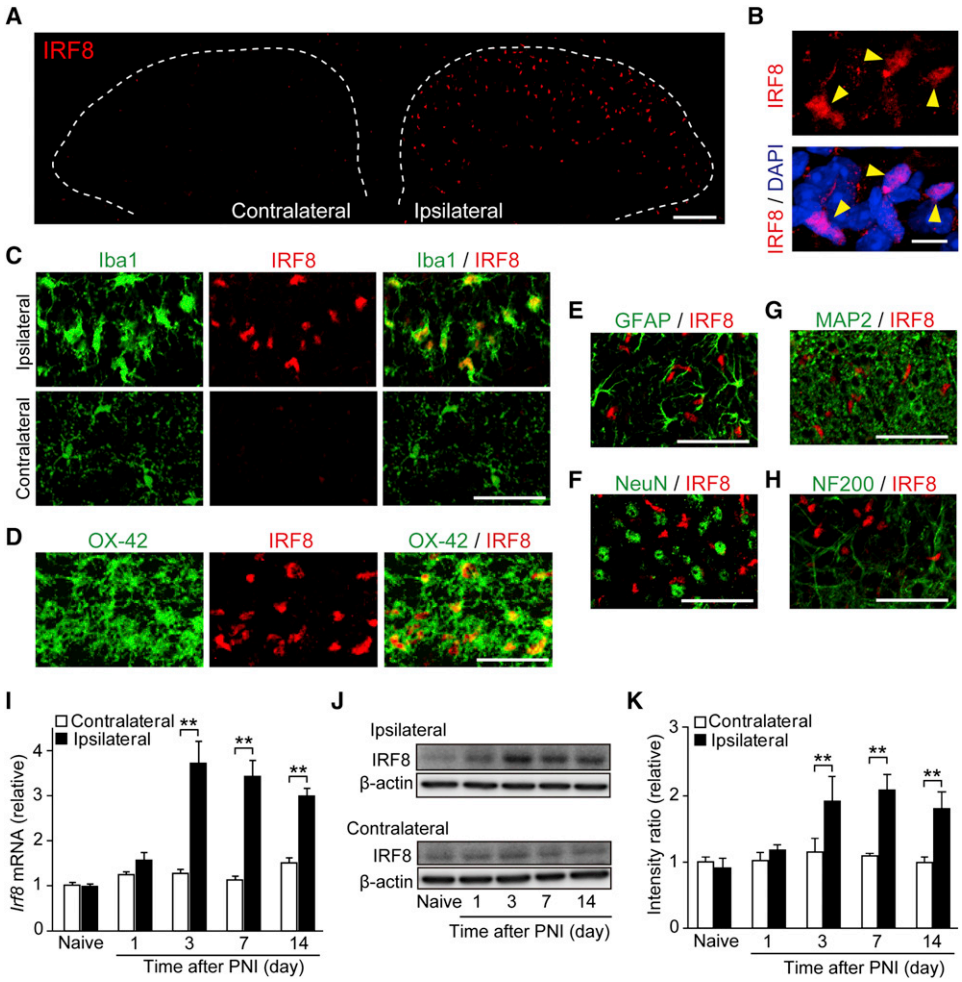

Figure 1. PNI Induces IRF8 Upregulation Exclusively in Microglia in the Spinal Cord

(A) Visualization of IRF8 protein in the dorsal spinal cord 3 days after PNI.

(B) Nuclear localization of IRF8.

(C–H) Double immunolabeling of IRF8 with Iba1 (C), OX-42 (D), GFAP (E), NeuN (F), MAP2 (G), and NF200 (H).

(I) Real-time PCR analysis of *Irf8* mRNA in WT mouse spinal cord before (Naive) and after PNI. Values represent the relative ratio of *Irf8* mRNA (normalized to *Gapdh* mRNA) to the contralateral side of naive mice (n = 6; **p < 0.01).

(J) Western blot analysis of IRF8 protein in the spinal cords of WT mice before (Naive) and after PNI.

(K) A histogram of the relative band density ratio of IRF8 (normalized to β-actin) to the contralateral side of naive mice at each time point (n = 5; **p < 0.01). Values are means ± SEM for all groups.

Scale bars: 100 μm (A), 10 μm (B), 50 μm (C–H).

See also Figure S1.

(Figure S1B). At higher magnification, almost all IRF8 immunofluorescence colocalized with the nuclear marker DAPI (Figure 1B). We further performed double-immunolabeling with cell type-specific markers and found that almost all IRF8$^+$ cells were positive for the microglial markers Iba1 (328/332 IRF8$^+$ cells; Figure 1C) and OX-42 (363/368 IRF8$^+$ cells; Figure 1D). IRF8$^+$ cells were not double-labeled with markers for neurons (NeuN, MAP2, and NF200) or astrocytes (GFAP) (Figures 1E–1H). By triple labeling with IRF8/Iba1/DAPI, we confirmed the nuclear localization of IRF8 in microglia (Figure S1C). Spinal microglia with the high levels of IRF8 showed activated morphology (Figure 1C), and the intensity of IRF8 immunofluorescence per Iba1$^+$ cell was markedly increased (Figures S1E and S1F). We therefore concluded that, in the dorsal horn following PNI, reactive microglia are the cell type which express IRF8 and that the level of IRF8 expression is dramatically increased in individual reactive microglia. In addition, microglia-specific IRF8 upregulation in the spinal cord was also induced in rats after PNI (Figures S1K–S1O). Furthermore, we examined the temporal pattern of IRF8 expression by real-time RT-PCR analysis and found that *Irf8* mRNA levels, which were low in naive mice, were increased in the spinal cord ipsilateral to PNI, starting from postoperative day 1 and peaking on day 3 and persisting for more than 3 weeks (Figure 1I; Figure S1D). Correspondingly, western blot analysis

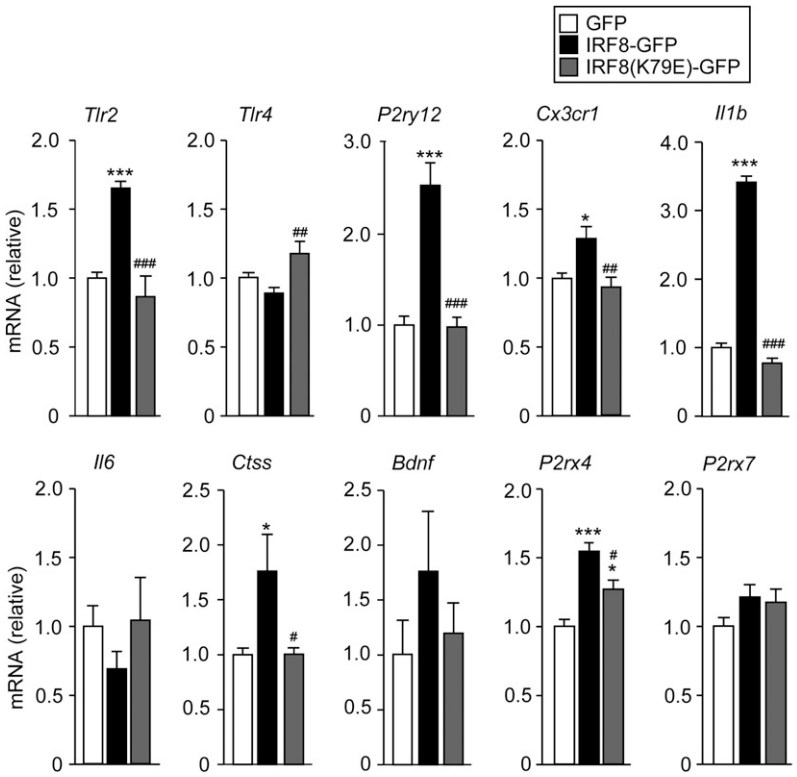

Figure 2. Forced Expression of IRF8 in Microglia Promotes Gene Transcription

Real-time PCR analysis of the mRNA of genes of interest in cultured microglia 72 hr after transduction. Values represent the relative ratio of mRNA (of tested genes, normalized to *Gapdh* mRNA) to control microglia with GFP alone (n = 5–7, $^{*}p < 0.05$, $^{***}p < 0.001$ versus GFP; $^{\#}p < 0.05$, $^{\#\#}p < 0.01$, $^{\#\#\#}p < 0.001$ versus IRF8-GFP). Values are the mean ± SEM for all groups.
See also Figure S2.

demonstrated upregulation of IRF8 protein in the ipsilateral spinal cord after PNI (Figures 1J and 1K). Spinal IRF8 upregulation at both earlier (24–44 hr) and later (days 7–21) time points after PNI was also specific to microglia (Figures S1G–S1J), indicating that the microglia-specific upregulation of IRF8 persists for at least 3 weeks after PNI.

To determine if IRF8 activates transcription in microglia, we transduced primary cultured microglia with a lentiviral vector encoding IRF8 tagged with green fluorescent protein (GFP) (IRF8–GFP) or a control vector encoding GFP alone, and examined the levels of gene transcripts in microglia. On the basis of current concepts that there are multiple activity states of reactive microglia (Hanisch and Kettenmann, 2007; Perry et al., 2010; Ransohoff and Cardona, 2010), we focused on genes involved in microglial innate responses (TLR2 [*Tlr2*] and TLR4 [*Tlr4*]) (Rivest, 2009), chemotaxis (the metabotropic nucleotide receptor P2Y12R [*P2ry12*] and the chemokine receptor CX3CR1 [*Cx3cr1*]) (Haynes et al., 2006; Honda et al., 2001; Tran and Miller, 2003) and inflammatory components (IL-1β [*Il1b*], IL-6 [*Il6*], cathepsin S [*Ctss*], brain-derived neurotrophic factor [*Bdnf*], the ionotropic nucleotide receptors P2X4R [*P2rx4*], and P2X7R [*P2rx7*]) (Burnstock, 2008; Clark et al., 2007; Coull et al., 2005; Inoue and Tsuda, 2009; Tsuda et al., 2003). First, we confirmed transduction efficacy of the two vectors (Figures S2A and S2B) and the *Irf8* mRNA level in microglia with IRF8–GFP (Figure S2C). In IRF8-transduced microglia, the mRNA levels for *Tlr2*, *P2ry12*, *Cx3cr1*, *Il1b*, *Ctss*, and *P2rx4* were increased (Figure 2). We confirmed similar effects of IRF8 using the microglial cell line BV2 (Figures S2D and S2E). *Bdnf* mRNA tended to be increased (Figure 2), and mRNAs for *Tlr4*, *Il6*, and *P2rx7* were not altered by IRF8 overexpression (Figure 2). Furthermore, in microglia transduced with a mutant IRF8 in which lysine at amino acid position 79 (required for DNA-binding activity; Tamura et al., 2000) was replaced with Glu (IRF8[K79E]), expression of genes that were induced by wild-type IRF8 was not increased (Figure 2). The failure of the mutant protein to induce gene expression was not due to insufficient levels of mutant IRF8 (Figure S2C). Thus, forced IRF8 expression activates transcription of genes associated with a reactive state of microglia in a manner that depends on its ability to bind DNA.

To investigate the role of IRF8 in microglial gene expression in vivo, we subjected *Irf8*$^{-/-}$ mice and their wild-type (WT) littermates to PNI and examined the abundance of microglial gene transcripts in the spinal cord. Based on our findings in vitro (Figure 2), we focused on putative IRF8-regulated microglial genes. In WT mice, the transcript levels of *Tlr2*, *P2ry12*, *Cx3cr1*, *Il1b*, *Ctss*, and *P2rx4* were significantly increased 7 days after PNI (Figure 3A). However, in *Irf8*$^{-/-}$ mice, the PNI-induced increase in expression of *Tlr2*, *P2ry12*, *Cx3cr1*, *Ctss*, and *Bdnf* was suppressed, and *P2rx4* and *Il1b* mRNAs did not significantly increase after PNI (Figure 3A). These results indicate that IRF8 is necessary for PNI-induced expression of a set of genes in reactive microglia in vivo. In addition, we examined gene expression at a later time point. On day 21 post-PNI, we found, in WT mice, a significant increase for the genes *Tlr2*, *Cx3cr1*, and *Ctss* in addition to Iba1 (*Aif1*) (Figures S3D and S3E). However, like *Irf8* mRNA on day 21 (Figure S1D), their levels were lower than those on day 7. Among them, the upregulation of *Ctss* and *Aif1* mRNAs was significantly suppressed in *Irf8*$^{-/-}$ mice (Figure S3D). The lesser effects of IRF8 deficiency on microglial gene expression might be related to the lower level of IRF8 in microglia on day 21 post-PNI.

Robust proliferation of spinal microglia is an early event occurring after PNI and is an important process for transforming into a reactive state (Tsuda et al., 2009). Thus, it is possible that the impaired microglial gene expression in *Irf8*$^{-/-}$ mice may be due to a change in this early process. However, PNI-induced increases in the number of proliferating spinal microglia that were positive for the proliferation markers Ki-67 and phosphorylated-histone H3 (p-HisH3) were indistinguishable between WT and *Irf8*$^{-/-}$ mice (Figure 3B). Furthermore, increased

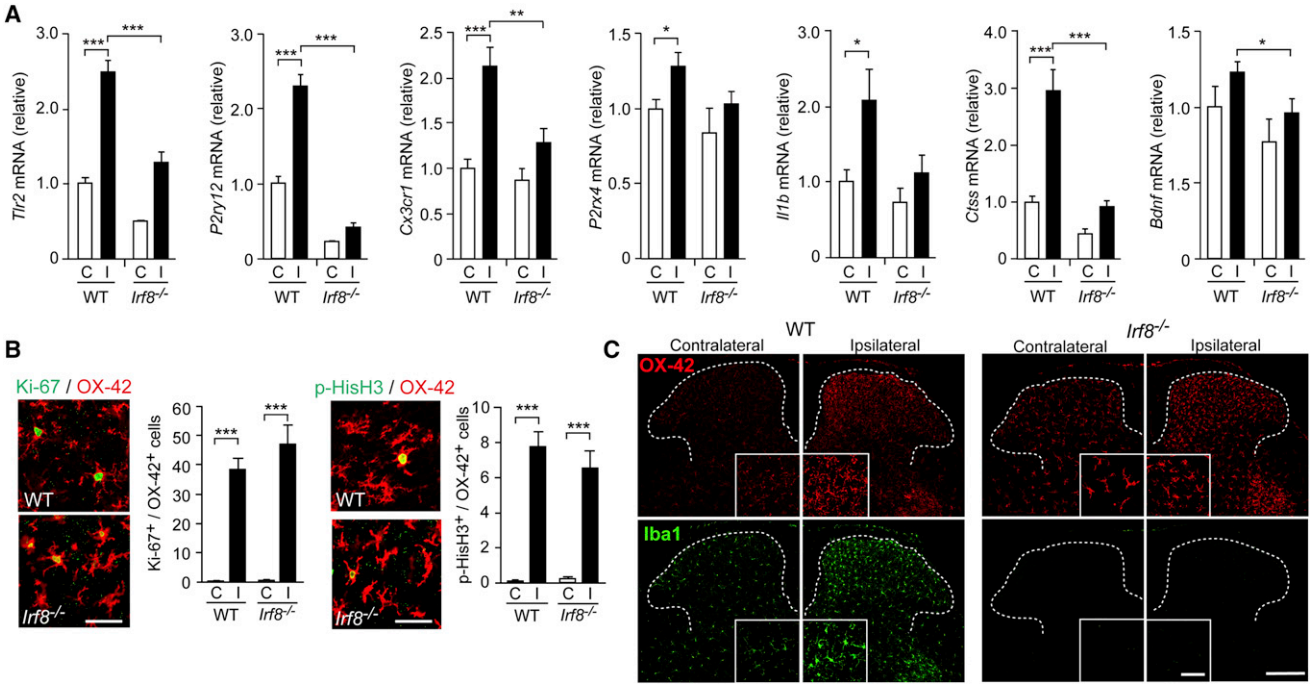

Figure 3. IRF8 Is Required for Microglial Gene Expression, but Not for Microglial Proliferation, in the Spinal Cord after PNI

(A) Real-time PCR analysis of mRNAs of microglial genes in the spinal cords of WT and *Irf8*$^{-/-}$ mice 7 days after PNI. Values represent the relative ratio of mRNA (of tested genes, normalized to *Gapdh* mRNA) to the contralateral side of WT mice. C, contralateral; I, ipsilateral. (n = 6–7, *p < 0.05, **p < 0.01, ***p < 0.001).

(B) Double immunofluorescence for Ki-67 or p-HisH3 (green) and OX-42 (red) in the ipsilateral dorsal horn of WT or *Irf8*$^{-/-}$ mice 2 days after PNI. A histogram of the numbers of Ki-67^{+}OX-42^{+} or p-HisH3^{+}OX-42^{+} cells in the ipsilateral (I) and contralateral (C) dorsal horn (n = 3, ***p < 0.001).

(C) OX-42 (red) and Iba1 (green) immunofluorescence in the spinal cord of WT and *Irf8*$^{-/-}$ mice 14 days after PNI.

Values are the mean ± SEM for all groups. Scale bars: 50 μm (B), 200 μm (C), 50 μm (C, insets).

See also Figure S3.

immunofluorescence of the microglial marker OX-42 after PNI, due to a cellular alteration of microglia, was similarly observed in the ipsilateral dorsal horn of both genotypes after PNI (Figure 3C). These data indicate that lack of IRF8 does not result in a global defect in reactive processes of microglia. However, *Irf8*$^{-/-}$ mice, surprisingly, showed a marked reduction in Iba1 immunofluorescence on both sides of the spinal cord (Figure 3C), which was also verified by real-time RT-PCR (Figures S3A and S3D) and Western blotting (Figure S3B). By using *Irf8*$^{+/-}$ mice, we showed that the reduction was dependent on levels of the *Irf8* gene (Figure S3C). The low level of *Aif1* mRNA was also observed in cultured *Irf8*$^{-/-}$ microglia (Figure S3F) and, conversely, was increased in cultured microglia transduced with IRF8, but not with IRF8(K79E) (Figures S3G and S3H). As there are IRF elements in the promoter region of the Iba1 gene (Sibinga et al., 2002), IRF8 may directly control Iba1 expression in microglia.

Our results above show that IRF8 is crucial for activating gene expression in reactive microglia in the spinal dorsal horn after PNI, raising the possibility that IRF8 might contribute to neuronal pathologies following PNI. Injury to the nervous system arising from bone compression in cancer, diabetes, infection, autoimmune disease or physical injury is known to result in debilitating chronic pain states (referred to as neuropathic pain) (McMahon and Malcangio, 2009; Tsuda et al., 2005). A cardinal symptom of neuropathic pain is characterized by tactile allodynia, abnormal pain hypersensitivity evoked by innocuous stimuli. Therefore, we investigated whether IRF8 induced in spinal microglia after PNI contributes to neuropathic allodynia using *Irf8*$^{-/-}$ mice. In WT mice, PNI produced a profound, long-term decrease in paw withdrawal threshold (PWT) to mechanical stimulation of the hindpaw (Figure 4A). The decrease in PWT on day 1 was comparable between WT and *Irf8*$^{-/-}$ mice, but *Irf8*$^{-/-}$ mice failed to show a further decrease in PWT after 3 days, lasting until the final time point tested. *Irf8*$^{-/-}$ mice showed no change in basal mechanical sensitivity or contralateral PWT after PNI (Figure 4A), nor did it affect motor function (data not shown). Furthermore, suppressing upregulated expression of spinal IRF8 after PNI by intrathecal administration of a small interfering RNA (siRNA) targeting IRF8, given on day 5 and 6 post-PNI to WT mice that had developed allodynia, caused a significant recovery in PWT (Figure 4B). Another IRF8 siRNA also produced similar effects (Figure S4F). Together, these data indicate that IRF8 upregulation in the spinal cord is necessary for full development and maintenance of tactile allodynia after PNI.

To further investigate the impact of microglial IRF8 in modulating pain, we employed a model in which cultured microglial cells are transferred spinally to normal mice (Figure 4C) (Coull et al., 2005; Tsuda et al., 2003, 2009). Transferring microglia transduced with GFP alone did not produce any change in

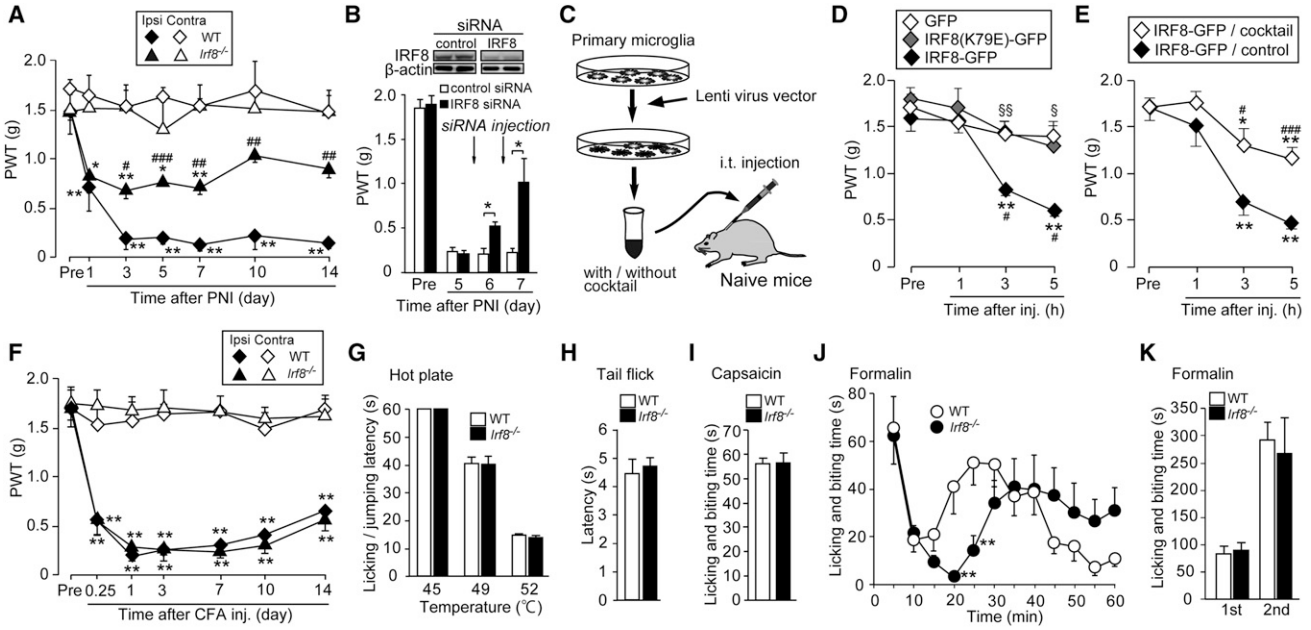

Figure 4. Microglial IRF8 Is Necessary for Abnormal Pain Hypersensitivity Caused by PNI

(A) PWT of *Irf8*$^{-/-}$ and WT mice before (Pre) and after PNI (n = 4; *p < 0.05, **p < 0.01 versus Pre; $^{\#}$p < 0.05, $^{\#\#}$p < 0.01, $^{\#\#\#}$p < 0.001 versus the ipsilateral side of WT mice). C, contralateral; I, ipsilateral.

(B) Reversal of PNI-induced allodynia by intrathecal administration of IRF8 siRNA (20 pmol) once a day for 2 days (on 5 and 6 days post-PNI) in WT mice (n = 3–6, *p < 0.05). Upper, representative immunoblots of IRF8 and β-actin proteins in the spinal cords of mice treated with control and IRF8 siRNAs on day 7 post-PNI.

(C) Experimental protocol.

(D) PWT of WT mice intrathecally administered with cultured microglia overexpressing either GFP, IRF8–GFP or IRF8(K79E)–GFP (n = 5–6, **p < 0.01 versus Pre; $^{\#}$p < 0.05 versus WT mice with GFP microglia; §p < 0.05, §§p < 0.01 versus WT mice with IRF8–GFP microglia).

(E) Allodynia by IRF8-transduced cultured microglia was prevented by preincubating microglia with a cocktail of IL-1β neutralizing antibody (5 μg) and CatS inhibitor (5 pmol) for 15 min before the intrathecal injection of microglia (n = 6–7, *p < 0.05, **p < 0.01 versus Pre; $^{\#}$p < 0.05, $^{\#\#\#}$p < 0.001 versus IRF8–GFP/control group).

(F) PWT of WT and *Irf8*$^{-/-}$ mice before (Pre) and after intraplantar CFA injection (n = 5, **p < 0.01 versus Pre).

(G) Hot-plate test. Values represent the latency (s) for animals to lick their hindpaws or jump (n = 6).

(H) Tail-flick test. Values represent the latency (s) to flick their tail from the heat source (n = 4).

(I–K) Capsaicin (I) and formalin (J and K) test. Values are the duration (s) of nociceptive behaviors (I: n = 6, J: n = 8) (**p < 0.01 versus WT mice). (K) Total duration (s) of nociceptive behaviors for 0–5 min (first phase) and for 10–60 min (second phase).

Values are the mean ± SEM for all groups.

See also Figure S4.

PWT (Figure 4D). By contrast, spinal transfer of IRF8-transduced microglia to normal mice produced a significant decrease in PWT (Figure 4D). However, IRF8(K79E)-transduced microglia failed to decrease PWT (Figure 4D). It is possible that transferring IRF8-transduced microglia may activate endogenous spinal IRF8 in recipient mice, leading to allodynia. However, IRF8-transduced microglia also produced behavioral allodynia in *Irf8*$^{-/-}$ mice (n = 3, pre: 1.50 ± 0.25 g; 5 hr: 0.58 ± 0.04 g). Thus, microglial IRF8 is sufficient to produce tactile allodynia, the behavioral outcome depends on the DNA-binding activity of IRF8. Microglia-mediated inflammatory components are implicated in enhancing neuronal excitability in the CNS including the dorsal horn (Inoue and Tsuda, 2009; Kawasaki et al., 2008; McMahon and Malcangio, 2009). Because gene transcripts upregulated by IRF8 included *IL1b* and *Ctss* (Figure 2), we tested the effect of these two inflammatory molecules in behavioral allodynia elicited by IRF8-expressing microglia. We found that pretreating IRF8-transduced microglia with a cocktail containing a function-blocking antibody for IL-1β and an inhibitor of Ctss attenuated the decrease in PWT by IRF8-transduced microglia (Figure 4E). Thus, these results imply that inflammatory signals derived from microglia overexpressing IRF8 can produce behavioral allodynia.

Because *Irf8*$^{-/-}$ mice may have congenital defects in pain processing, we also tested behavioral responses in other pain assays. Intraplantar injection of complete Freund's adjuvant (CFA), a model of pain caused by local inflammation of the hindpaw, produced no detectable change in spinal IRF8 expression (Figure S4G) and caused pain hypersensitivity in both WT and *Irf8*$^{-/-}$ mice (Figure 4F). In acute pain assays, behavioral responses to heat and capsaicin were indistinguishable between the two genotypes (Figures 4G–4I). Likewise, pain responses related to tissue damage by injecting dilute formalin into the hindpaw did not differ, although *Irf8*$^{-/-}$ mice showed a delay in onset of the second phase (Figures 4J and 4K). By using several markers for DRG neurons, we confirmed that the phenotypes of

DRG neurons are comparable between the two genotypes (Figures S4A–S4E). Thus, microglial IRF8 critically contributes to chronic pain, especially neuropathic pain, without causing substantial alterations in basal sensory thresholds, local tissue inflammation-induced pain or motor performance.

Here, we demonstrate a role for IRF8 in the CNS as a key transcription regulator of microglia involved in converting to a reactive state after PNI in vivo. To our knowledge, IRF8 is the first transcription factor specific to microglia, among CNS-resident cells, that controls their reactive processes and CNS pathology. We further found that IRF8 upregulation in brain microglia was also observed in other models of injury (hypoglossal nerve axotomy and kainic acid-induced neuronal injury) (Figures S1P–S1R), suggesting that upregulation of microglial IRF8 may be commonly induced following diverse types of neuronal injury. Interestingly, IRF8 deficiency prevented gene expressions in microglia without affecting their proliferative activity. Therefore, our findings suggest that IRF8 is not the sole transcription factor for microglial activation but rather activates a program of gene expression that determines signaling activity of reactive microglia, which provides a newly observed mechanism for microglial activation. For the IRF8 upregulation in microglia, it has been reported that interferon (IFN)-γ increases IRF8 expression in vitro (Politis et al., 1994) and IFN-γ receptors are expressed in spinal microglia (Tsuda et al., 2009). However, we found that IFN-γ receptor-deficient mice failed to prevent PNI-induced *Irf8* expression in the spinal cord (Figure S1S), proposing the possible involvement of an IFN-γ-independent mechanism (e.g., TLRs; Barber et al., 1995). Although elucidating this issue requires further investigation, our present data suggest that inhibiting upregulated expression or function of IRF8 may provide a way to comprehensively control the expression of a set of genes in reactive microglia. Of importance to therapeutic development, *Irf8*$^{-/-}$ mice were resistant to allodynia, and suppressing spinal IRF8 by its siRNA reversed established allodynia. Although the possible involvement of other cell types expressing IRF8 in neuropathic pain defects seen in *Irf8*$^{-/-}$ mice cannot be excluded, our findings indicate that the development and maintenance of neuropathic pain requires ongoing activity of microglial IRF8. Therefore, our results may provide a new therapeutic strategy for neuropathic pain, for which there is currently no effective therapy. In addition, reactive microglia with altered expression of various genes by an as-yet-unknown mechanism play prominent roles in the pathogenesis of other CNS diseases (Glass et al., 2010; Hanisch and Kettenmann, 2007; Perry et al., 2010). A recent meta-analysis identified *IRF8* as a susceptibility locus for multiple sclerosis (De Jager et al., 2009), a refractory neurodegenerative disease in which reactive microglia are implicated (Glass et al., 2010). Whether reactive microglia upregulate IRF8 expression and its transcriptional activity during the course of CNS diseases remains unknown. However, if so, then this transcription factor could provide a therapeutic target in disorders of the CNS in addition to neuropathic pain.

EXPERIMENTAL PROCEDURES

Details are further described in the Extended Experimental Procedures.

Animals

Male IRF8-deficient mice (*Irf8*$^{-/-}$) (Holtschke et al., 1996) and their WT littermates, and C57BL/6 mice were used. All mice used were aged 9–12 weeks at the start of each experiment and were housed at 22 ± 1°C with a 12-hr light-dark cycle and fed food and water ad libitum. All experimental procedures were performed under the guidelines of Kyushu University.

Peripheral Nerve Injury

Under isoflurane (2%) anesthesia, a unilateral L4 spinal nerve of mice was cut as described previously (Tsuda et al., 2009).

Microarray Analysis

Total RNA from the L3–L5 spinal cord was converted to biotin-labeled cRNA, which was hybridized to the Mouse WG-6 V2.0 BeadChip (Illumina). Gene expression was analyzed according to BeadStudio Gene Expression Module User Guide (Illumina).

Quantitative Real-Time PCR

Quantitative PCR was performed with Premix Ex *Taq* (Takara) using a 7500 real-time PCR system (Applied Biosystems), and the data were analyzed using 7500 System SDS Software 1.3.1.

Western Blot and Immunohistochemistry

Western blot and immunohistochemistry were performed using standard methods. See Supplemental Information for details.

Microglial Culture

Mouse primary cultured microglia were prepared as described previously (Tsuda et al., 2003, 2009).

Lentiviral Transduction

The lentiviral CS2-EF-MCS vector expressing mouse IRF8-GFP, IRF8(K79E)-GFP (Tamura et al., 2000), or GFP alone were used. Viral particles were added onto primary cultured microglia (1.2×10^5 cells/well). Total RNA in cultured microglia 72 hr after the transduction were used for real-time PCR analysis. For behavioral tests, the transduced microglia were washed, harvested, and administering intrathecally to catheterized mice.

Intrathecal Administration

Intrathecal injection of IRF8 siRNA (20 pmol/5 μl) and cultured microglia (2×10^4 cells/5 μl) was followed by infusion of 3 μl of PBS. Fifteen minutes before the injection of transduced microglia, cells were mixed with a reagent cocktail (5 μL) containing an IL-1β neutralizing antibody (5 μg, R&D Systems) and the CatS inhibitor Z-FL-COCHO (5 pmol, Calbiochem), or with a control vehicle.

Behavioral Studies

To assess mechanical sensitivity, calibrated von Frey filaments (0.02–2.0 g) were applied to the plantar surfaces of the hindpaws of mice, and the 50% PWT was determined. Methods for all other tests are described in the Supplemental Information.

Statistical Analysis

Statistical analyses were performed using the Student's t test (Figures 4B, 4G–4I, and 4K), two-way ANOVA with post hoc Bonferroni test (Figures 1I, 1K, 4A, 4F, and 4J), one-way ANOVA with a post hoc Dunnett's test (Figures 4A and 4D–4F), or Tukey's test (Figures 2, 3A, 3B, 4D, and 4E) using GraphPad Prism 4.03 software. Differences were considered significant at $p < 0.05$.

SUPPLEMENTAL INFORMATION

Supplemental Information includes Extended Experimental Procedures and four figures and can be found with this article online at doi:10.1016/j.celrep.2012.02.014.

LICENSING INFORMATION

ACKNOWLEDGMENTS

This work was supported by grants from the JSPS through the NEXT Program initiated by the CSTP (M.T.) and the MEXT of Japan (T.M., M.T., K.I.) and from the Core-to-Core program of JSPS (K.I.). We thank Ms. Junko Kitano, Ms. Yukari Hasegawa, Dr. Shigeo Hasegawa and the Research Support Center (Graduate School of Medical Sciences, Kyushu University) for assisting with experiments, and Dr. Hiroyuki Miyoshi (RIKEN BioResource Center) for providing the lentiviral vector and its packaging plasmids. T.M. designed and performed most of the experiments, analyzed the data, and wrote the manuscript. M.T. conceived the study, supervised the overall project, performed immunohistochemical experiments, and wrote the manuscript. R.Y. assisted with the experiments. H.T.-S. optimized transduction of lentiviral vectors into primary cultured microglia. K.O. and T.T. provided critical materials including *Irf8*$^{-/-}$ mice and advice on data interpretation. K.I. supervised the overall project and wrote the manuscript.

Received: October 7, 2011
Revised: February 13, 2012
Accepted: February 29, 2012
Published online: April 5, 2012

REFERENCES

Barber, S.A., Fultz, M.J., Salkowski, C.A., and Vogel, S.N. (1995). Differential expression of interferon regulatory factor 1 (IRF-1), IRF-2, and interferon consensus sequence binding protein genes in lipopolysaccharide (LPS)-responsive and LPS-hyporesponsive macrophages. Infect. Immun. *63*, 601–608.

Burnstock, G. (2008). Purinergic signalling and disorders of the central nervous system. Nat. Rev. Drug Discov. *7*, 575–590.

Clark, A.K., Yip, P.K., Grist, J., Gentry, C., Staniland, A.A., Marchand, F., Dehvari, M., Wotherspoon, G., Winter, J., Ullah, J., et al. (2007). Inhibition of spinal microglial cathepsin S for the reversal of neuropathic pain. Proc. Natl. Acad. Sci. USA *104*, 10655–10660.

Coull, J.A., Beggs, S., Boudreau, D., Boivin, D., Tsuda, M., Inoue, K., Gravel, C., Salter, M.W., and De Koninck, Y. (2005). BDNF from microglia causes the shift in neuronal anion gradient underlying neuropathic pain. Nature *438*, 1017–1021.

De Jager, P.L., Jia, X., Wang, J., de Bakker, P.I., Ottoboni, L., Aggarwal, N.T., Piccio, L., Raychaudhuri, S., Tran, D., Aubin, C., et al; International MS Genetics Consortium. (2009). Meta-analysis of genome scans and replication identify CD6, IRF8 and TNFRSF1A as new multiple sclerosis susceptibility loci. Nat. Genet. *41*, 776–782.

Glass, C.K., Saijo, K., Winner, B., Marchetto, M.C., and Gage, F.H. (2010). Mechanisms underlying inflammation in neurodegeneration. Cell *140*, 918–934.

Hanisch, U.K., and Kettenmann, H. (2007). Microglia: active sensor and versatile effector cells in the normal and pathologic brain. Nat. Neurosci. *10*, 1387–1394.

Haynes, S.E., Hollopeter, G., Yang, G., Kurpius, D., Dailey, M.E., Gan, W.B., and Julius, D. (2006). The P2Y12 receptor regulates microglial activation by extracellular nucleotides. Nat. Neurosci. *9*, 1512–1519.

Holtschke, T., Löhler, J., Kanno, Y., Fehr, T., Giese, N., Rosenbauer, F., Lou, J., Knobeloch, K.P., Gabriele, L., Waring, J.F., et al. (1996). Immunodeficiency and chronic myelogenous leukemia-like syndrome in mice with a targeted mutation of the ICSBP gene. Cell *87*, 307–317.

Honda, K., and Taniguchi, T. (2006). IRFs: master regulators of signalling by Toll-like receptors and cytosolic pattern-recognition receptors. Nat. Rev. Immunol. *6*, 644–658.

Honda, S., Sasaki, Y., Ohsawa, K., Imai, Y., Nakamura, Y., Inoue, K., and Kohsaka, S. (2001). Extracellular ATP or ADP induce chemotaxis of cultured microglia through Gi/o-coupled P2Y receptors. J. Neurosci. *21*, 1975–1982.

Inoue, K., and Tsuda, M. (2009). Microglia and neuropathic pain. Glia *57*, 1469–1479.

Kawasaki, Y., Zhang, L., Cheng, J.K., and Ji, R.R. (2008). Cytokine mechanisms of central sensitization: distinct and overlapping role of interleukin-1beta, interleukin-6, and tumor necrosis factor-alpha in regulating synaptic and neuronal activity in the superficial spinal cord. J. Neurosci. *28*, 5189–5194.

McMahon, S.B., and Malcangio, M. (2009). Current challenges in glia-pain biology. Neuron *64*, 46–54.

Perry, V.H., Nicoll, J.A., and Holmes, C. (2010). Microglia in neurodegenerative disease. Nat. Rev. Neurol. *6*, 193–201.

Politis, A.D., Ozato, K., Coligan, J.E., and Vogel, S.N. (1994). Regulation of IFN-gamma-induced nuclear expression of IFN consensus sequence binding protein in murine peritoneal macrophages. J. Immunol. *152*, 2270–2278.

Ransohoff, R.M., and Cardona, A.E. (2010). The myeloid cells of the central nervous system parenchyma. Nature *468*, 253–262.

Rivest, S. (2009). Regulation of innate immune responses in the brain. Nat. Rev. Immunol. *9*, 429–439.

Sibinga, N.E., Feinberg, M.W., Yang, H., Werner, F., and Jain, M.K. (2002). Macrophage-restricted and interferon gamma-inducible expression of the allograft inflammatory factor-1 gene requires Pu.1. J. Biol. Chem. *277*, 16202–16210.

Tamura, T., Nagamura-Inoue, T., Shmeltzer, Z., Kuwata, T., and Ozato, K. (2000). ICSBP directs bipotential myeloid progenitor cells to differentiate into mature macrophages. Immunity *13*, 155–165.

Tamura, T., Yanai, H., Savitsky, D., and Taniguchi, T. (2008). The IRF family transcription factors in immunity and oncogenesis. Annu. Rev. Immunol. *26*, 535–584.

Tran, P.B., and Miller, R.J. (2003). Chemokine receptors: signposts to brain development and disease. Nat. Rev. Neurosci. *4*, 444–455.

Tsuda, M., Shigemoto-Mogami, Y., Koizumi, S., Mizokoshi, A., Kohsaka, S., Salter, M.W., and Inoue, K. (2003). P2X4 receptors induced in spinal microglia gate tactile allodynia after nerve injury. Nature *424*, 778–783.

Tsuda, M., Inoue, K., and Salter, M.W. (2005). Neuropathic pain and spinal microglia: a big problem from molecules in "small" glia. Trends Neurosci. *28*, 101–107.

Tsuda, M., Masuda, T., Kitano, J., Shimoyama, H., Tozaki-Saitoh, H., and Inoue, K. (2009). IFN-gamma receptor signaling mediates spinal microglia activation driving neuropathic pain. Proc. Natl. Acad. Sci. USA *106*, 8032–8037.

Cell PRESS
Open ACCESS

EXTENDED EXPERIMENTAL PROCEDURES

Peripheral Nerve Injury

We used the spinal nerve injury model (Kim and Chung, 1992) with some modifications (Tsuda et al., 2009b) in 9- to 12-week-old mice. Under isoflurane (2%) anesthesia, a small left-side incision at L3–S1 was made. Paraspinal muscle and fat were removed from the L5 traverse process, and the part of this traverse process was removed to expose the parallel-lying L3 and L4 spinal nerves. The L4 nerve was carefully isolated and cut. For rats, the L5 spinal nerve was tightly ligated by a 5-0 silk suture and cut just distal to the ligature (Tsuda et al., 2003). The wound was sutured with 5-0 silk. The surrounding skin was pulled together and sutured with 5-0 silk.

Hypoglossal Nerve Transection

Under isoflurane (2%) anesthesia, an unilateral axotomy of dorsal motor neurons of the vagus (DMV) neurons was made by cutting the right vagal bundle at the neck along the vagus nerve (Gowing et al., 2006). The wound was sutured with 5-0 silk. The surrounding skin was pulled together and sutured with 5-0 silk.

Kainic Acid-Induced Neuronal Injury

Intraperitoneal injection of kainic acid (KA; 20 mg/kg) dissolved in PBS was used to induce a status epilepticus in 9- to 12-week-old mice (Avignone et al., 2008), and age-matched PBS-injected animals were used as control. Forty-eight hours after the KA injection, mice were deeply anesthetized and perfused with 4% paraformaldehyde. Brains were removed and used for immunohistochemical analysis.

Quantitative Real-Time PCR

Mice were deeply anesthetized with pentobarbital, perfused transcardially with PBS, and the L3–L5 spinal cord was removed immediately. The tissues were vertically separated by median, and hemisections of the spinal cord were subjected to total RNA extraction using Trisure (Bioline) according to the protocol of the manufacturer and purified with RNeasy mini plus kit (QIAGEN, Valencia, CA). Extraction of total RNA from primary cultured microglia or the microglial cell line BV-2 (provided by Dr. Knut Biber, University of Freiburg) was also performed using TRIsure. The amount of total RNA was quantified by measuring OD_{260} using a Nanodrop spectrophotometer (Nanodrop, Wilmington, DE). For reverse transcription, 100 ng of total RNA was transferred to the reaction with Prime Script reverse transcriptase (Takara). Quantitative PCR was performed with Premix Ex *Taq* (Takara) using a 7500 real-time PCR system (Applied Biosystems), and the data were analyzed using 7500 System SDS Software 1.3.1 (Applied Biosystems). Expression levels were normalized to the values for GAPDH (glyceraldehyde-3-phosphate dehydrogenase), then results were presented relative to those of WT contralateral side (Figures 1H and 3A), or control microglia cells treated with GFP-coding viral particles (Figure 2). The sequences of TaqMan primer pairs and probe are described below.

Mouse IRF8: 5′-GGATATGCCGCCTATGACACA-3′ (forward), 5′-CATCCGGCCCATACAACTTAG-3′ (reverse), 5′-FAM-CCATTCAGCTTTCTCCCAGATGGTCATC-TAMRA-3′ (probe)
Rat IRF8: 5′- CGCACACCATTCAGCCTTATCCCAG-3′ (forward),
5′-TGGTGACTGGGTATACTGCCTATG-3′ (reverse),
5′-FAM-TGCCCCCGTAGTAAAAGTTGA-TAMRA-3′ (probe)
TLR2: 5′-CCCTTCTCCTGTTGATCTTGCT-3′ (forward), 5′-CGCCCACATCATTCTCAGGTA-3′ (reverse), 5′-FAM-CTGTGCCACCATTTCCACGGACTG -TAMRA-3′ (probe)
TLR4: 5′-AAACTTGCCTTCAAAACCTGGC-3′ (forward), 5′-ACCTGAACTCATCAATGGTCACATC-3′ (reverse), 5′-FAM-CACGTCCATCGGTTGATCTTGGGAGAA-TAMRA-3′ (probe)
CX3CR1: 5′-TCACCGTCATCAGCATCGA-3′ (forward), 5′-CTGCACTGTCCGGTTGTTCA-3′ (reverse),
5′-FAM-ATCGTCCTGGCCGCCAACTCC -TAMRA-3′ (probe)
P2X4R: 5′-ACAACGTGTCTCCTGGCTACAAT-3′ (forward), 5′-GTCAAACTTGCCAGCCTTTCC-3′ (reverse), 5′-FAM-CAATGAGCAACGCACACTCACCAAGG-TAMRA-3′ (probe)
P2X7R: 5′-TGCAGCTGGAACGATGTCTT-3′ (forward), 5′-CCAAAGCAAAGCTCTAATGTAGGAA-3′ (reverse), 5′-FAM-TATGAGACAAACAAAGTCACCCGGATCCA-TAMRA-3′ (probe)
P2Y12R: 5′-TGAAGACCACCAGGCCATTT-3′ (forward), 5′-AGGCCCAGATGACAACAGAAA-3′ (reverse), 5′-FAM-AAACGTCCAGCCCCAGCAATCTCTTG-TAMRA-3′ (probe)
IL-1β: 5′-GAAAGACGGCACACCCACC-3′ (forward), 5′-AGACAAACCGCTTTTCCATCTTC-3′ (reverse), 5′-FAM-TGCAGCTGGAGAGTGTGGATCCCAA-TAMRA-3′ (probe)
IL-6: 5′-GGGACTGATGCTGGTGACAA-3′ (forward), 5′-TGCCATTGCACAACTCTTTTCT-3′ (reverse), 5′-FAM-TCACAGAGGATACCACTCCCAACAGACCTG-TAMRA-3′ (probe)
BDNF: 5′-GCCCAACGAAGAAAACCATAAG-3′ (forward), 5′-TGTTTGCGGCATCCAGGTA-3′ (reverse), 5′-FAM-CACTTCCCGGGTGATGCTCAGCA-TAMRA-3′ (probe)
Cathepsin S: 5′-TACATTCAGCTCCCGTTTGGT-3′ (forward), 5′-TCGTCATAGACACCGCTTTTGT-3′ (reverse), 5′-FAM-TCGACGCCAGCCATTCCTCCTTCT-TAMRA-3′ (probe),

Iba1 (*Aif1*): 5′-GATTTGCAGGGAGGAAAAGCT-3′ (forward), 5′-AACCCCAAGTTTCTCCAGCAT-3′ (reverse), 5′-FAM-CAGGAAGA GAGGCTGGAGGGGATCAA-TAMRA-3′ (probe)

as well as the primers and probe for GAPDH, were obtained from Applied Biosystems.

Western Blotting

Mice were deeply anesthetized with pentobarbital, perfused transcardially with PBS, and the L3–L5 spinal cord was removed immediately. For rats, the L4–L6 spinal cord was used. The tissues were vertically separated by median, and then hemisections of the spinal cord were homogenized in homogenization buffer (20 mM Tris-HCl [pH 7.4], 2 mM EDTA, 0.5 mM EGTA, 0.32 M sucrose, protease, and phosphatase inhibitors cocktails) for 10 s on ice and centrifuged at 1,000*g* for 10 min at 4°C to remove cell debris. The supernatant was transferred to a new tube, mixed with Laemmli sample buffer and boiled at 95°C for 5 min. Then, the samples were subjected to a 10% polyacrylamide gel, and the proteins were transferred electrophoretically to PVDF membranes (GE Healthcare). The membrane was blocked with Blocking One (Nacalai tesque), and was incubated with anti-IRF8 antibody (1:500, Santa Cruz), anti-Iba1 antibody (ionized calcium-binding adaptor molecule-1, 1:500, Wako) or anti-β-actin antibody (1:2000, Sigma) overnight at 4°C. The antibodies were detected using HRP-conjugated secondary antibody (1:1000, GE Healthcare). The blots were detected using an ECL Western blotting detection system (GE Healthcare) and a LAS-3000 imaging system (Fujifilm). For densitometric quantification, the relative band density of IRF8 to β-actin was quantified using the software NIH Image J 1.36, and the values for IRF8 were normalized to the values of β-actin for the loading control.

Immunohistochemistry

Mice and rats were deeply anesthetized by pentobarbital and perfused transcardially with phosphate-buffered saline (PBS, composition in mM: NaCl 137, KCl 2.7, KH_2PO_4 1.5, NaH_2PO_4 8.1; pH 7.4) followed by ice-cold 4% paraformaldehyde/PBS. The L4 (mice) or L5 (rats) segment of the lumbar spinal cord, or the L4 segments of the dorsal root ganglion (DRG) were removed, postfixed in the same fixative, and placed in 30% sucrose solution for 24 hr at 4°C. Transverse L4 or L5 spinal cord sections (30 μm) or L4 DRG sections (15 μm) were cut on a Leica CM 1850 cryostat and incubated for 2 hr at room temperature in a blocking solution (3% normal goat or donkey serum), and then incubated for 48 hr at 4°C in the primary antibody for IRF8 (1:500, Santa Cruz), TRPV1 (transient receptor potential cation channel subfamily V member 1, 1:500, Santa Cruz), P2X3R (1:2500, Chemicon), CGRP (calcitonin gene-related peptide, 1:4000, Peninsula Laboratories) and parvalbumin (1:500, Swant). Identification of cell types was performed using the following markers: microglia, OX-42 (1:1000, Serotec) and Iba1 (1:2000, Wako); astrocytes, GFAP (glial fibrillary acidic protein, 1:500, Chemicon); neurons, NeuN (Neuronal Nuclei, 1:200, Chemicon), MAP2 (microtubule-associated protein 2, 1:1000, Chemicon) and NF200 (neurofilament 200, 1:400, Sigma). To visualize proliferating cells, two proliferation markers, Ki-67 (1:10000, Novocastra) and phospho-histone H3 (Ser10) (1:1000, Millipore), were used. Spinal sections were incubated with secondary antibodies conjugated to Alexa Fluor 488 or 546 (1:1000, Molecular Probes) and mounted in VECTASHIELD with or without DAPI (Vector Laboratories). Three to five sections from the L4 spinal cord segments of each mouse were randomly selected and analyzed using an LSM510 Imaging System (Carl Zeiss Japan). The numbers of Ki-67$^+$ or p-HisH3$^+$ microglia with an S/N ratio of 3.0 or more were counted. For the size-frequency analyses, measurement of the cross-sectional areas of Nissl-stained neurons (total DRG neurons), TRPV1-, P2X3R-, CGRP- or parvalbumin-positive neurons was made by using an LSM Image Browser (Zeiss) and only neurons with clearly visible nuclei were used for the quantification.

Microglial Culture

Mouse primary cultured microglia were prepared as described previously (Nakajima et al., 1992; Tsuda et al., 2003, 2009b). Briefly, a mixed glial culture was prepared from neonatal mice and maintained for 10–16 days in DMEM with 10% fetal bovine serum. Immediately before experiments, microglia were collected by a gentle shake as the floating cells over the mixed glial culture. The microglia were transferred to dishes for subsequent experiments. The cultures were of >99% purity.

Lentiviral Transduction

Full-length cDNAs for mouse IRF8–GFP, IRF8(K79E)–GFP(Tamura et al., 2000), and GFP alone were cloned into the lentiviral CS2-EF-MCS vector (RIKEN). Each vector with pCAG-HIVgp (packaging plasmid; RIKEN), and pCMV-VSV-G-RSV-Rev (RIKEN) was cotransfected into HEK293T cells. After mixing with PEG, viral particles and 8 μg/ml polybrene were added onto primary cultured microglia plated on 24-well plates (1.2×10^5 cells/well). After a 12 hr treatment with the lentivirus, cultured medium was changed to conditioned medium prepared from the mixed glial culture, and microglia were further cultured for 60 hr. For the gene expression experiments, the transduced microglia were subjected to total RNA extraction as described above. The transcriptional effects of IRF8-GFP fusion protein has been confirmed to be identical to IRF8 (Laricchia-Robbio et al., 2005). In addition, we also confirmed that the ability to increase in the *Aif1* mRNA expression is not indistinguishable between IRF8 and IRF8-GFP-transduced BV2 microglial cells (Figure S3H).

Intrathecal Catheterization

Under isoflurane (2%) anesthesia, mice were implanted with a 32-gauge intrathecal catheter (ReCathCo, Allison Park, PA) through the atlanto-occipital region and in the lumbar enlargement (close to L3–L4 segments) of the spinal cord. After 7 days recovery, the

catheter placement was verified by the observation of transient hindpaw paralysis induced by intrathecal injection of lidocaine (2%, 1.5 μl). Animals that failed to show any paralysis were not used in experiments.

Behavioral Studies

To assess mechanical sensitivity, mice were placed individually in an opaque plastic cylinder, which was placed on a wire mesh and habituated for 1 hr to allow acclimatization to the new environment. After that, calibrated von Frey filaments (0.02–2.0 g, North Coast Medical) were applied to the plantar surfaces of the hindpaws of mice with or without intrathecally administered transduced microglia, PNI, or peripheral inflammation caused by intraplantar injection of CFA (0.01 mg/20 μl, Sigma), and the 50% PWT was determined using the up-down method (Chaplan et al., 1994). In a hot-plate test, mice were placed on a metal surface maintained at 45, 49 or 52°C within a 25-cm-high Plexiglas box (25 cm^2). The latency to either lick or shake the hindpaw or jump was measured as a nocifensive end point (Cao et al., 1998). Noxious heat-evoked tail flick responses were detected by the application of radiant heat (Ugo Basile, Italy) to the tail. The intensity of the heat stimulus was adjusted to 50 V, and the latency of the tail withdrawal response (seconds) was measured (Tsuda et al., 2007). In a capsaicin test, mice were placed individually in individual box and allowed to habituate to the testing environment (15 min). After that, 10 μl of capsaicin (1.0 μg/paw, 1.0% DMSO) was injected intraplantarly in the ventral surface of the left hind paw. Animals were observed individually for 5 min. The amount of time spent licking and biting the injected paw was recorded and was considered as indicative of nociception (Tsuda et al., 2009a). In the tests of formalin-induced pain, mice were housed in individual box and allowed to habituate to the testing environment for 15 min. Then, mice were injected intraplantarly with formalin (5%, 20 μl), and then the duration of the licking and biting responses to the injected hindpaw was recorded at 5 min intervals for 60 min after the injection (formalin pain) (Tsuda et al., 2007).

SUPPLEMENTAL REFERENCES

Avignone, E., Ulmann, L., Levavasseur, F., Rassendren, F., and Audinat, E. (2008). Status epilepticus induces a particular microglial activation state characterized by enhanced purinergic signaling. J. Neurosci. *28*, 9133–9144.

Cao, Y.Q., Mantyh, P.W., Carlson, E.J., Gillespie, A.M., Epstein, C.J., and Basbaum, A.I. (1998). Primary afferent tachykinins are required to experience moderate to intense pain. Nature *392*, 390–394.

Chaplan, S.R., Bach, F.W., Pogrel, J.W., Chung, J.M., and Yaksh, T.L. (1994). Quantitative assessment of tactile allodynia in the rat paw. J. Neurosci. Methods *53*, 55–63.

Gowing, G., Vallières, L., and Julien, J.P. (2006). Mouse model for ablation of proliferating microglia in acute CNS injuries. Glia *53*, 331–337.

Kim, S.H., and Chung, J.M. (1992). An experimental model for peripheral neuropathy produced by segmental spinal nerve ligation in the rat. Pain *50*, 355–363.

Laricchia-Robbio, L., Tamura, T., Karpova, T., Sprague, B.L., McNally, J.G., and Ozato, K. (2005). Partner-regulated interaction of IFN regulatory factor 8 with chromatin visualized in live macrophages. Proc. Natl. Acad. Sci. USA *102*, 14368–14373.

Nakajima, K., Shimojo, M., Hamanoue, M., Ishiura, S., Sugita, H., and Kohsaka, S. (1992). Identification of elastase as a secretory protease from cultured rat microglia. J. Neurochem. *58*, 1401–1408.

Tamura, T., Nagamura-Inoue, T., Shmeltzer, Z., Kuwata, T., and Ozato, K. (2000). ICSBP directs bipotential myeloid progenitor cells to differentiate into mature macrophages. Immunity *13*, 155–165.

Tsuda, M., Shigemoto-Mogami, Y., Koizumi, S., Mizokoshi, A., Kohsaka, S., Salter, M.W., and Inoue, K. (2003). P2X4 receptors induced in spinal microglia gate tactile allodynia after nerve injury. Nature *424*, 778–783.

Tsuda, M., Ishii, S., Masuda, T., Hasegawa, S., Nakamura, K., Nagata, K., Yamashita, T., Furue, H., Tozaki-Saitoh, H., Yoshimura, M., et al. (2007). Reduced pain behaviors and extracellular signal-related protein kinase activation in primary sensory neurons by peripheral tissue injury in mice lacking platelet-activating factor receptor. J. Neurochem. *102*, 1658–1668.

Tsuda, M., Kuboyama, K., Inoue, T., Nagata, K., Tozaki-Saitoh, H., and Inoue, K. (2009a). Behavioral phenotypes of mice lacking purinergic P2X4 receptors in acute and chronic pain assays. Mol. Pain *5*, 28.

Tsuda, M., Masuda, T., Kitano, J., Shimoyama, H., Tozaki-Saitoh, H., and Inoue, K. (2009b). IFN-gamma receptor signaling mediates spinal microglia activation driving neuropathic pain. Proc. Natl. Acad. Sci. USA *106*, 8032–8037.

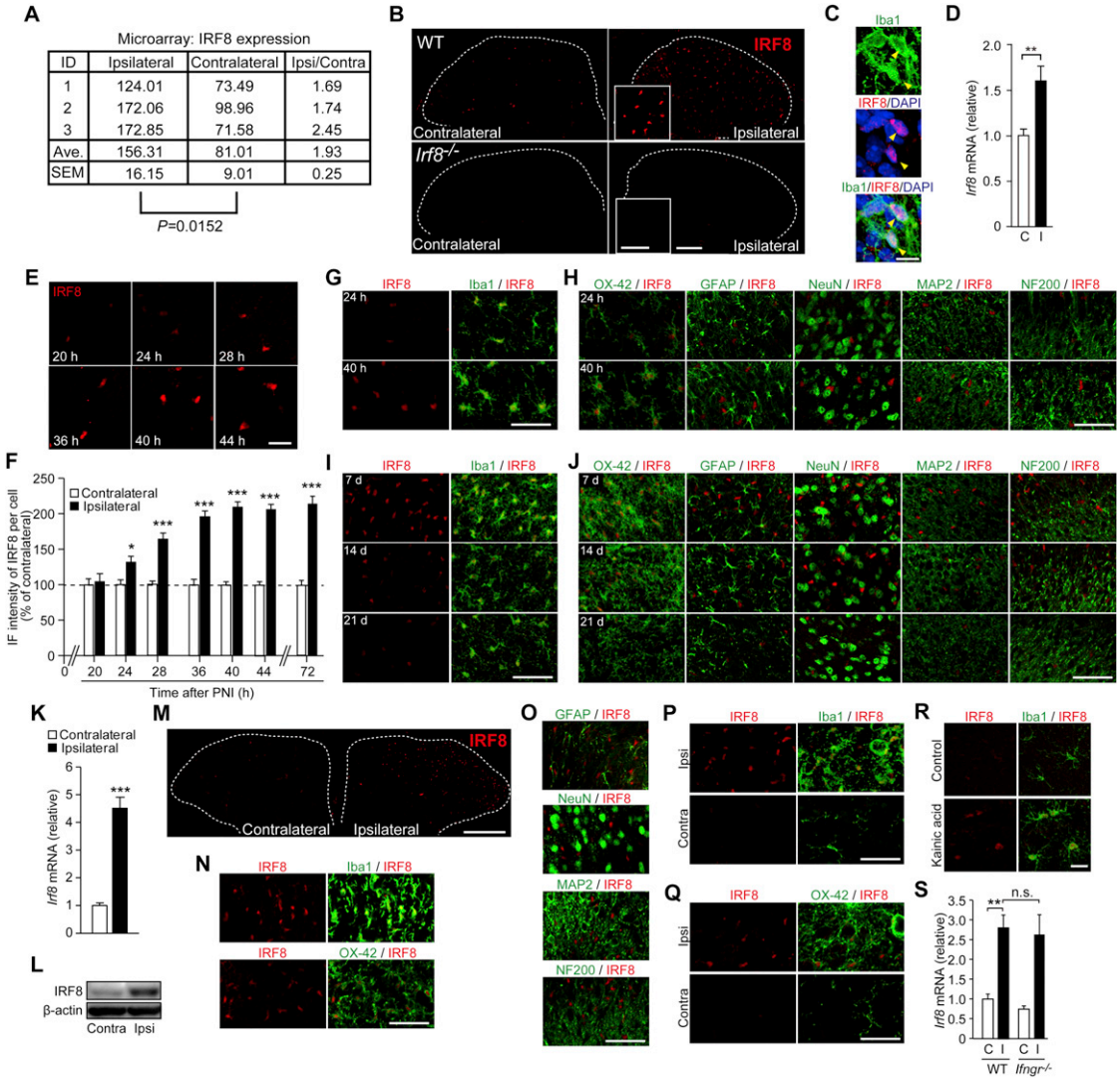

Figure S1. Microglia-Specific IRF8 Upregulation following PNI and Other Forms of Neuronal Injury, Related to Figure 1

(A) *Irf8* expression in the spinal cord 7 days after PNI by three independent DNA microarray analyses. (n = *3*; p = 0.015, Student's t test)

(B) Visualization of IRF8 protein in the dorsal horn of WT and *Irf8*$^{-/-}$ mice 3 days after PNI. (scale bar, 100 μm; insets, 50 μm).

(C) Triple-labeling with IRF8/Iba1/DAPI 3 days after PNI. (scale bar, 10 μm)

(D) Real-time PCR analysis of *Irf8* mRNAs in the spinal cord of WT mice on day 21 post-PNI. Values represent the relative ratio of mRNA (normalized to *Gapdh* mRNA) to the contralateral side. (n = 6, $^{**}p < 0.01$, Student's t test).

(E) IRF8 immunofluorescence in the dorsal horn of WT mice 20, 24, 28, 36, 40 and 44 hr after PNI (scale bar, 20 μm).

(F) The relative immunofluorescent (IF) intensity ratio of IRF8 to the contralateral side of WT mice at each time point (n = 16–99; $^{*}p < 0.05$, $^{***}p < 0.001$, Student's t test).

(G–J) Double immunolabeling of IRF8 with cell-type markers in the dorsal horn of WT mice 24 and 40 hr, and 7, 14, and 21 days after PNI. (scale bar, 50 μm).

(K) Real-time PCR analysis of *Irf8* mRNA in the rat spinal cord 7 days after PNI. Values represent the relative ratio of *Irf8* mRNA (normalized to *Gapdh* mRNA) to the contralateral side (n = 5; $^{***}p < 0.001$, Student's t test).

(L) Western blot analysis of IRF8 protein in the rat spinal cord on day 7.

(M) IRF8 immunofluorescence in the rat dorsal horn on day 7. (scale bar, 200 μm).

(N, O) Double immunolabeling of IRF8 with cell type markers in the rat dorsal horn on day 7. (scale bar, 50 μm).

(P, Q) Double immunolabeling of IRF8 with Iba1 and OX-42 in the hypoglossal nucleus of WT mice 7 days after hypoglossal nerve axotomy. (scale bar, 50 μm)

(R) Double immunolabeling of IRF8 with Iba1 in the hippocampal of WT mice 48 hr after intraperitoneal administration of kainic acid (20 mg/kg) or vehicle (Control). (scale bar, 20 μm)

(S) Real-time PCR analysis of *Irf8* mRNAs in the spinal cords of WT and IFN-γ receptor- deficient (*Ifngr*$^{-/-}$) mice 3 days after PNI. Values represent the relative ratio of *Irf8* mRNA (normalized to the value for *Gapdh* mRNA) to the contralateral side of WT mice. (n = 5; $^{**}p < 0.01$, one-way ANOVA with Tukey's multiple comparison test). Values are the mean ± SEM for D, F, K and S.

Contra or C, contralateral; Ipsi or I, ipsilateral.

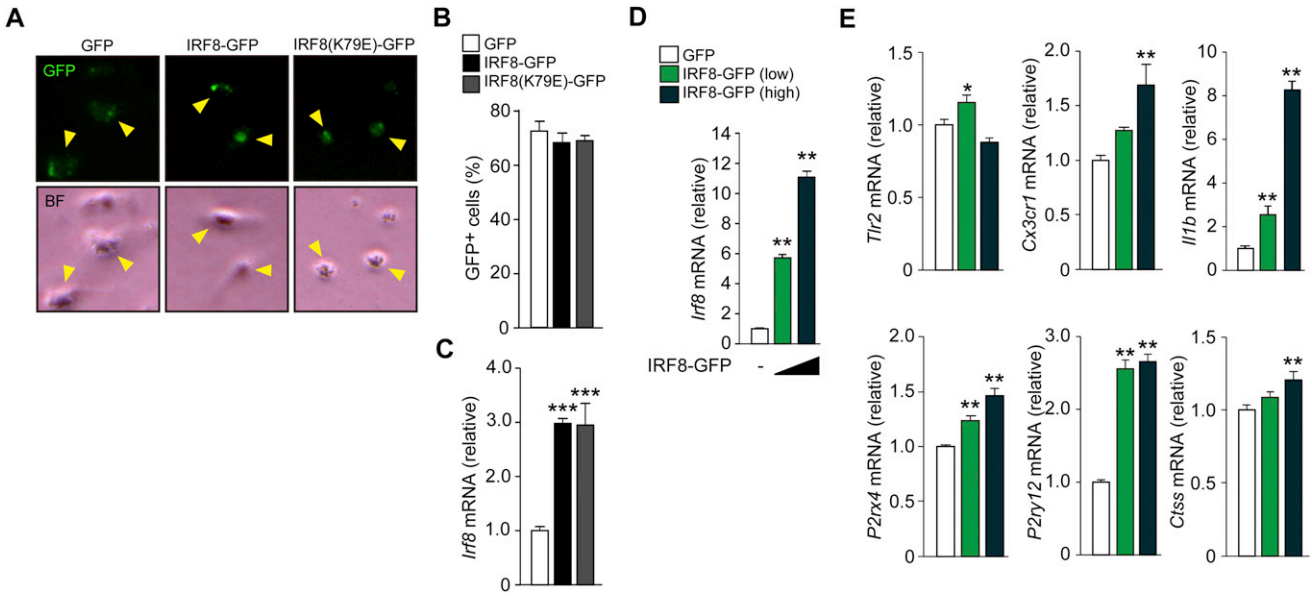

Figure S2. Lentiviral-Mediated IRF8 Transduction into Cultured Microglia, Related to Figure 2

(A) GFP or bright field (BF) images of primary cultures of microglia transduced with a lentiviral vector encoding either IRF8 in conjunction with GFP (IRF8-GFP), mutant IRF8(K79E)-GFP, or control GFP alone (GFP).

(B) Percentage of GFP^+ cells in total microglia cells 72 hr after the transduction. (n = 6).

(C) *Irf8* mRNA in cultured microglia 72 hr after the transduction. (n = 7, $***p < 0.001$ versus GFP, one-way ANOVA with Tukey's multiple comparison test).

(D and E) mRNA of *Irf8* (D) and microglial genes (E) in BV2 cells 72 hr after the transduction with IRF8-GFP (high or low dose) or GFP alone. (D, E; n = 8, $*p < 0.05$; $**p < 0.01$ versus GFP, one-way ANOVA with Dunnett's multiple comparison test).

For the (C)–(E), values indicate the ratio of *Irf8* mRNA/*Gapdh* mRNA, normalized to the GFP microglia.

Values are the mean ± SEM for (B)–(E).

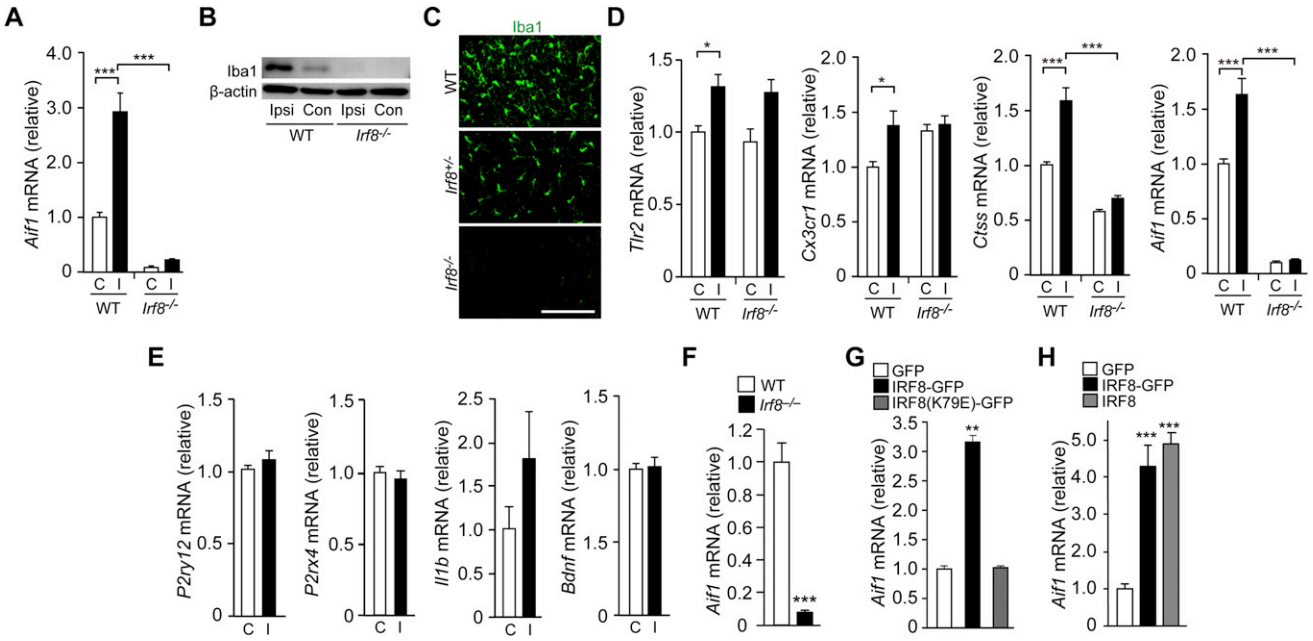

Figure S3. IRF8 Regulates Microglial Gene Expression, Related to Figure 3

(A) Real-time PCR analysis of *Aif1* mRNAs in the spinal cords of WT and *Irf8*$^{-/-}$ mice 7 days after PNI. (n = 6–7, ***p < 0.001, one-way ANOVA with Tukey's multiple comparison test).

(B) Western blot analysis of Iba1 protein in the spinal cords of WT and *Irf8*$^{-/-}$ mice 7 days after PNI.

(C) Iba1 immunofluorescence in the dorsal horn of WT, *Irf8*$^{+/-}$ and *Irf8*$^{-/-}$ mice 14 days after PNI. (scale bar, 100 μm)

(D) Real-time PCR analysis of mRNAs of microglial genes in the spinal cords of WT and *Irf8*$^{-/-}$ mice on day 21 after PNI. (n = 4–6, *$p < 0.05$, **$p < 0.01$, ***$p < 0.001$, one-way ANOVA with Tukey's multiple comparison test).

(E) *P2ry12*, *P2rx4*, *Il1b* and *Bdnf* mRNAs in the spinal cord of WT mice on day 21 (n = 6).

(F) *Aif1* mRNA in primary microglia isolated from WT and *Irf8*$^{-/-}$ mice. (n = 5–6, ***$p < 0.001$ versus WT microglia, Student's t test).

(G and H) *Aif1* mRNA in BV2 cells 72 hr after lentiviral transduction. (n = 8, **$p < 0.01$, ***$p < 0.001$ versus GFP, one-way ANOVA with Tukey's multiple comparison test).

For the panels A, D and E, values represent the relative ratio of tested gene mRNA (normalized to *Gapdh* mRNA) to the contralateral side of WT or *Irf8*$^{-/-}$ mice. For the panels G and H, values indicate the ratio of *Aif1* mRNA/*Gapdh* mRNA, normalized to the GFP microglia.

Values are the mean ± SEM for (A) and (D)–(H).

C, contralateral; I, ipsilateral.

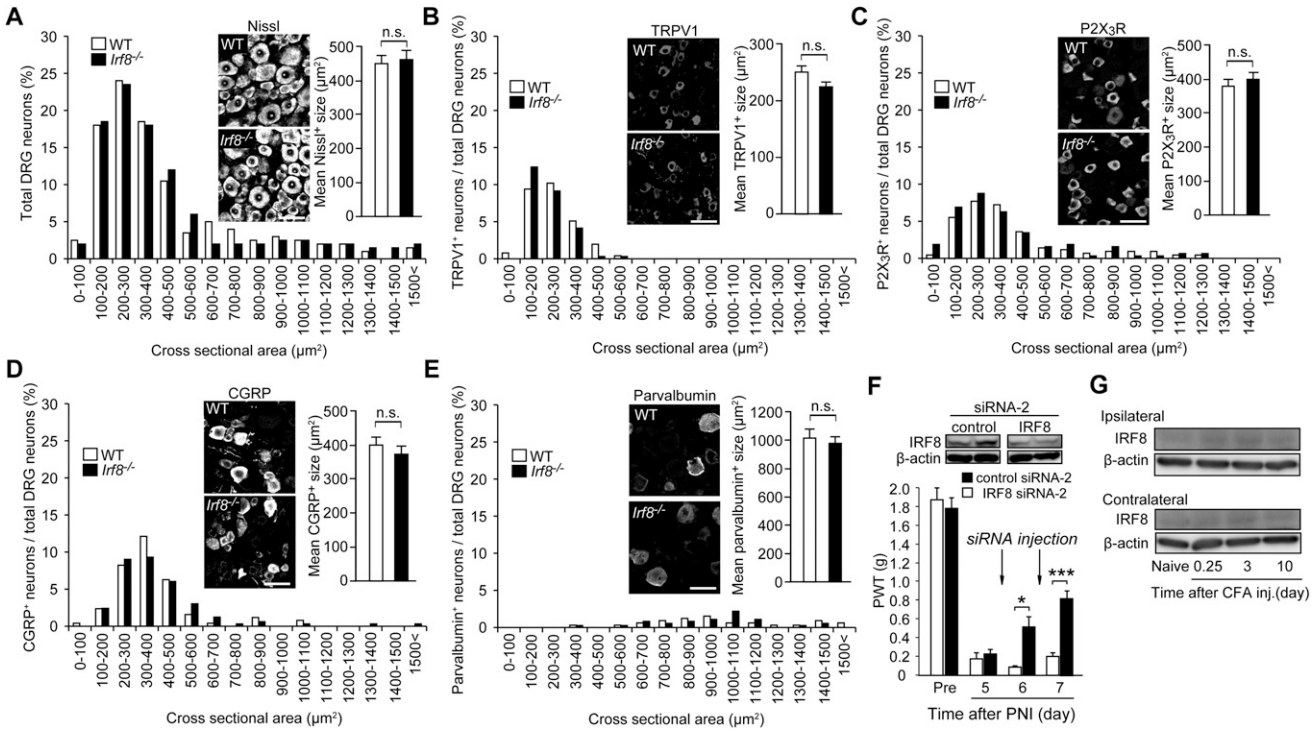

Figure S4. Phenotypes of Dorsal Root Ganglion Neurons Are Not Changed in IRF8-Deficient mice, Related to Figure 4

(A–E) Size-frequency histogram illustrating the distribution of the cross-sectional areas of dorsal root ganglion (DRG) neurons positive for Nissl (total) (A), TRPV1 (B), P2X3R (C), CGRP (D) and parvalbumin (E) in WT and *Irf8*$^{-/-}$ mice. Inset photographs: representative images of each marker. (scale bar, 50 μm). Inset histogram: mean somal area of DRG neurons positive for each marker. (Values are the mean ± SEM, n = 200–415, Student's t test)

(F) Reversal of PNI-induced tactile allodynia by intrathecal administration of IRF8 siRNA-2 (20 pmol) once a day for 2 days (5 and 6 days post-PNI) in WT mice. Values are the mean ± SEM (n = 3–6, $*p < 0.05$, $***p < 0.001$, Student's t test) Upper, representative immunoblots of IRF8 and β-actin protein in homogenates obtained from the spinal cord of mice treated with control and IRF8 siRNA-2 on day 7 post-PNI.

(G) Western blot analysis of IRF8 protein in the ipsilateral and contralateral spinal cords of WT mice before (Naive) and after intraplantar CFA injection.